Baryón anibaryónová asymmetria v centrálnej oblasti rapidity na LHC ALICE

Michal Broz

UNIVERZITA KOMENSKÉHO
FAKULTA MATEMATIKY FYZIKA A INFORMATIKY
KATEDRA JADROVEJ FYZIKY A BIOFYZIKY

Jadrová a subjadrová fyzika

Školiteľ: prof. RNDr. Branislav Sitár DrSc.

BRATISLAVA 2008

Baryon – antibaryon asymmetry in central rapidity region at LHC ALICE

Michal Broz

COMENIUS UNIVERSITY
FACULTY OF MATHEMATICS PHYSICS AND INFORMATICS
DEPARTMENT OF NUCLEAR PHYSICS AND BIOPHYSICS

Nuclear and Subnuclear Physics

Supervisor: prof. RNDr. Branislav Sitár DrSc.

BRATISLAVA 2008

Abstrakt

Broz Michal: Baryón anibaryónová asymmetria v centrálnej oblasti rapidity na LHC ALICE. Fakulta Matematiky, Fyziky a Informatiky Univerzita Komenského. Katedra Jadrovej Fyziky a Biofyziky. Bratislava, 2008. 44 strán.

Štúdium asymetrie počtu baryónov a antibaryónov v oblasti nízkych rapidít je kľúčové pre objasnenie charakteru nositeľov (prenášateľov) baryónového náboja pri zrážke. Skúmaný efekt vyvolaný charakterom nositeľov je malý a môže byť silno skreslený systematickými efektami sprevádzajúcimi rekonštrukciu dráh a identifikáciu častíc. Skúmanie účinnosti týchto procesov a vytvorenie korekcií na ne je cieľom tejto práce.

Abstract

Broz Michal: Baryon antibaryon asymmetry in central rapidity region at LHC ALICE. Faculty of Mathematics Physics and Informatics. Comenius University. Department of Nuclear Physics and Biophysics. Bratislava, 2008. 44 pages.

Study of asymmetry in number of baryons and antibaryons in central rapidity region is important for clarification of baryon number carriers character. Effect we are interested in is small, can be hidden by systematical processes of particle track reconstruction and identification. To make corrections on these effects is the aim of this thesis.

Contents

Introduction

It is not obvious which partons in the proton carry its baryon number. Naive approach leads to association of baroyn number with valence quarks. However, this assumption is not dictated by the structure of QCD, and therefore does not to be true. Probe to nature of baryon number in several situations leads to association of baryon number with special configuration of gluonic field inside of the baryon including so called string junction. These two theories can be tested experimentally by measuring the asymmetry of baryon number in central rapidity region.

In model where the baryon number of the incident proton is associated with valence quarks and transferred to a more central rapidity region by diquark exchange the mechanism is attenuated exponentially with the rapidity interval over which the baryon charge is moved. Alternatively, when baryon number is carried by gluonic field, baryon number flow can be due to a purely gluonic mechanism. This is accounted for in models where the three valence quarks of the proton fragment independent but are joined by strings to a baryonic gluon field configuration at more central rapidity, the so-called string junction. When the baryon number is carried by gluons, there will be nonzero asymmetry in central rapidity. “Real physics” is hidden by systematical effects – we need to study it and make correction to see reality.

The ALICE detector, with its particle-identification capabilities, is ideally suited to clarify this issue with abundant baryon statistics in several channels (p, Λ) in the central-rapidity region.

In this thesis we are studying effects of reconstruction and particle identification to multiplicity of identified protons. The goals are:

- To study asymmetry distributions produced from different monte carlo generators which can be expected on ALICE.
- To prepare the macro which will extract reconstruction efficiency and particle identification efficiency for protons and antiprotons respectively. Choose reasonable cuts which reflect abilities of ALICE detector.
- Use these efficiency maps to correct the simulated data. To show how it passed to monte carlo multiplicities of protons which represents “real physics”.

1 Baryon number

1.1 Baryon number carriers in baryon

It is not obvious which partons in the proton carry its baryon number. Really? In QCD, quarks carry colour, flavor electric charge and isospin. Naive approach leads to association of baroyn number with valence quarks. This consequence comes from the definition of baryon number of hadronic system. The definition is:

D: Baryon number of hadronic system is given by the number of quarks minus number of antiquarks divided by three.

Experimental fact is that baryon number is conserved in closed system. Density of valence quarks in a baryon of flavor *i* carrying a momentum fraction *x* is defined as

$$q_i^v(x) = q_i(x) - \overline{q_i}(x), \tag{1.1}$$

then

$$\sum_i \int_0^1 dx\left(q_i(x) - \overline{q_i}(x)\right) = \sum_i \int_0^1 dx.q_i^v(x) = 3, \tag{1.2}$$

which also motivates the association of baryon number with valence quarks. However, this later assumption is not dictated by the structure of QCD, and therefore does not to be true.

It looks pretty clear and right, but let`s look on this reaction

$$\pi^- + p \to \Omega^- + K^+ + 2K^0, \tag{1.3}$$

you can see that baryon number is conserved and reaction is able quark diagram for this reaction is:

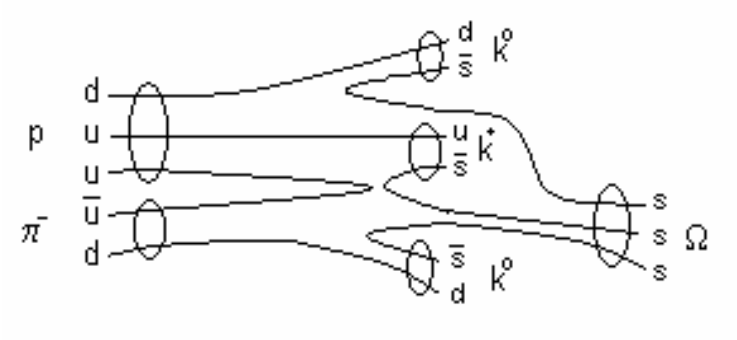

Figure 2.1: Quark diagram for the reaction (1.3). You can see that none of valence quarks in initial baryon appears as valence quark in final baryon

as you can see none of the valence quarks in the initial proton appear as valence quark in Ω^- . Thus baryon number must be carried by some other partons in the proton, probably gluons.

Another example which creates doubt that valence quarks carries baryon number is central colision of heavy ions. What happens through the collision? Substantial faction of coliding nuclei is stored in the valence quarks. We know that energy loss of quark propagating through a heavy nucleus is small and energy independent [21] [22] [23]. The number is $\Delta E \approx 10 GeV$. So high energy quark canot be stoped by soft interaction. The valence quarks pass through the collision region losing only small fraction of their energy on gluon radiation by soft collisions. So if valence quarks are cariers of baryon number, they will sweep the baryon number to fragmentation region. Many softer quark - antiquark pairs and gluons are left behind. After propagation through a heavy nucleus the initial valence quarks completly lse their identity as nucleon constituent. The fragmentation jets are created which consist mostly of mesons and a small number of baryon - antibaryon pairs. Therefore the baryon number carried by colliding nuclei is not to be found in the beam fragmentation region but is stuck in collision region. As you can see something is wrong. The valence quarks readily survive this collision and remain in

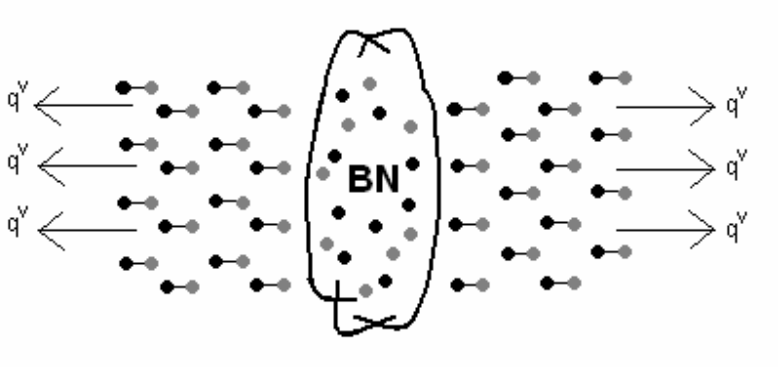

Figure 2.2: Picture illustrating final state folowing central collision of reativistic heavy nuclei. Grey and black circles coresponds to quarks and antiquarks. The valence quarks q^v escaping the collision region produced jets. Baryon number (BN) remains in collision region.

fragmentation regions while baryon number does not. Now the implication: Because the baryon number is stopped along with gluons it apears that gluon may carry the baryon number.

1.2 Nature of baryon number

1.2.1 The string configurations of the color fields in hadrons

The string configuration of the color fields in meson and in baryon are quite different. A meson looks like a quark - antiquark pair conected by a color flux tube [21]. Quark and antiquark are in state of color triplet, antitriplet respectively. The final color state of this configuration is given by color algebra:

$$\{3\} \otimes \{\bar{3}\} = \{1\} \oplus \{8\}, \tag{1.4}$$

where the color singlet is realized in nature. This fact is known as confinment of quarks in hadrons.

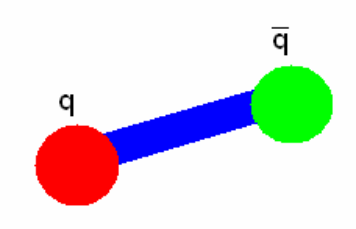

Figure 2.3: String configuration of meson

The configuration of strings in baryon having minimal energy has a form of the Mercedes - Benz star and the point where the strings joint is called the string junction [25]. One can imagine the parton cloud of a valence quark as quark - antiquark chain. In the baryon this valence quark is accompanied by valence diquark. The valence diquark is in a state of color antitriplet what is given by folowing equation

$$\{3\}\otimes\{3\}=\{\bar{3}\}\oplus\{6\}. \tag{1.5}$$

So the color state of diquark is the same as color state of antiquark. Diquark is accompanied with quark in a state of color triplet and final color state is also given by (1.4).

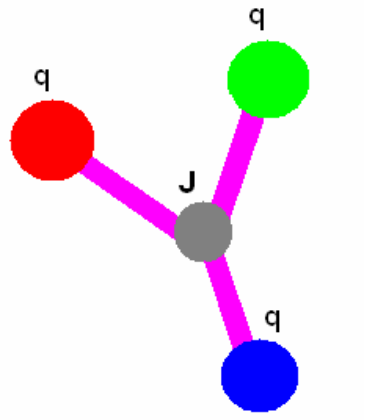

Figure 2.4: String configuration of baryon. The point where the strings joint is called string junction (J).

This was stable color states of baryon. Let`s look on the color states which can be created in hadronic colisions. These color state can be created in higher Fock components of baryon since Fock state decomposition of baryon contains components with few sea quark - antiquark pairs

$$|B\rangle = |3g^{v}\rangle + |3g^{v}q^{s}\bar{q}^{s}\rangle + |3g^{v}2q^{s}2\bar{q}^{s}\rangle..., \tag{1.6}$$

where color degrees of freedom of the sea quarks allow the valence configuration in non - singlet state. Interesting are these states: color octet and color decuplet.

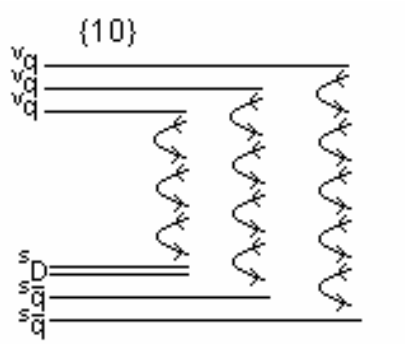

Figure 2.5: Decuplet color state {10} of baryon created in baryon Fock component $|3g^{v}2q^{s}2\bar{q}^{s}\rangle$. *Three valence quarks are accompanied by two sea antiquarks and sea diquark. Valence quarks are in decuplet state, but final state of full system are the color singlet what is implicated by (1.4).*

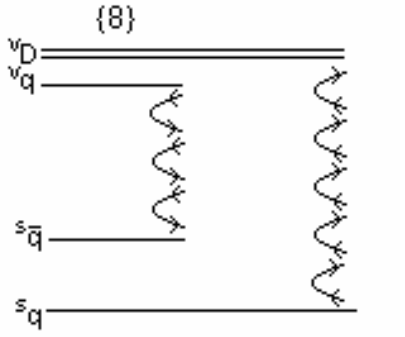

Figure 2.6: Octet color state {8} of baryon created in baryon Fock component $|3g^{v}q^{s}\bar{q}^{s}\rangle$. *Valence quark and valence diquark are accompanied by sea antiquark and sea quark respectively. Valence quarks are in octet state, but final state of full system are the color singlet what is implicated by (1.4).*

1.2.2 Annihilation of baryon number

Experiments on baryon number annihilation via $p + \bar{p} \rightarrow mesons$ were carried out in 1970. Important conclusion is that if baryon number is asociated with gluonic configuration, it will be rather uniformly distributed in rapidity and that the $p\bar{p}$ annihilation cross section will not vanish at high energy.

The first claim that the $p\bar{p}$ annihilation cross section is energy independent at high energies was made by Gotsman and Nussinov [24]. They employed a string junction model, and suggested that annihilation results from the overlap of gluonic string junction a string antijunction followed by rearrangement of the gluonic strings as is illustrated in Figure 7. They made a natural assumption that this process is energy independent in analogy to nonannihilation collisions corresponding to crossing of the strings. The annihilation cross section was estimated by assuming that string junction has a size of the order of the transverse dimension of the strings ~ *0.2 - 0.3 fm*. With this assumption they found $\sigma_{ann}^{\bar{p}p} \approx 1 - 2mb$.

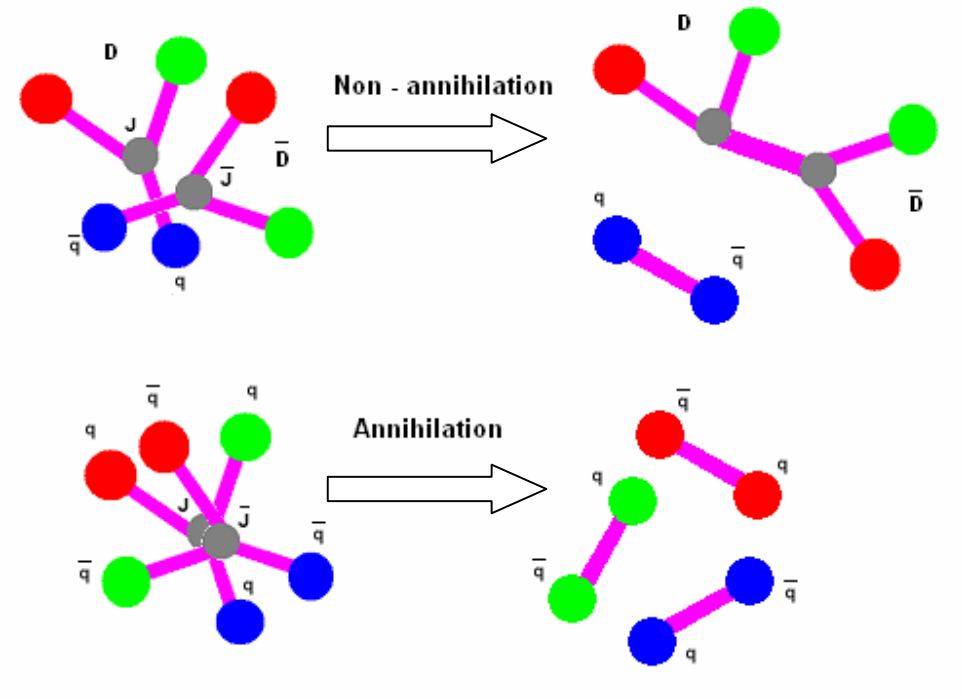

Figure 2.7: Picture shows interaction of a baryon consisted of diquark (D) and a quark with antibaryon. Crossing of the strings in the impact parameter plane leads to non - annihilation final state with two strings. Annihilation corresponds to overlap of string junction (J) with string antijunction ($\bar{J}$)leading to three string production

Figure 2.8: Baryon - antibaryon interaction once again. Picture shows three string final state which leads to annihilation (left) and two string, non - annihilation final state (right).

1.2.3 Baryon number asymetry of produced particles

Another probe of the baryon number distribution is the baryon number asymmetry of produced particles in hadron collision. Asymmetry can be defined as

$$A_{BN}(y) = 2\frac{N_{BN} - N_{\overline{BN}}}{N_{BN} + N_{\overline{BN}}}, \tag{1.7}$$

where $N_{BN}, N_{\overline{BN}}$ is the density of produced baryon, antibaryon number which is a function of rapidity *y*.

Let`s look on proton - photon (meson) collision. This is the case with initial baryon number equal one. It is natural to assume that baryon number asymmetry of produced particles arises from the baryon number asymmetry of the parton distribution in the projectil proton. One could expect an exponential attenuation of the baryon number flow over long rapidity interval and vanishing asymmetry at mid rapidities.

Source of baryon number asymmetry at mid rapidities can be understood in the parton model. In the infinite momentum frame of the proton one can attribute a partonic interpretation to the string junction since it carries a fraction of the proton momentum. In the rest frame of the proton all partons in the initial state of the γp interaction belong to the photon. Obviously the parton distribution of the photon is baryn number symetric. However, the interaction with the proton target breaks up this symmetry due the possibility of annihilation of anti baryon number in the projectile parton cloud of the photon with baryon number of the proton. This leads to non zero baryon number asymmetry in the final state. The rapidity distribution of the produced net baryon number is related to the energy behavior of the annihilation cross section. This reaction can go through two processes.

The valence quarks of target proton can occur in a state of color octet *{8}* and color decupled *{10}*. In process with participation of octet state the valence diquark is accompanied by quark from photon symmetric baryon fluctuation. Baryon has been made in the final state. Rapidity of this baryon is accompanied with rapidity of valence quarks. We can tell that baryon number was transfered from initial to final state what is related to the transfer thrugh rapidity interval between initial and final baryon. Dependence of

baryon number transfer on the rapidity interval Δy for this proces is proportial to $e^{-\frac{\Delta y}{2}}$ since it is related to the well known x - distribution of valence quarks dictated by Regge phenomenology. This proces is known as valence quark mechanism of baryon number transfer through rapidity interval and estimate vanishing baryon asymmetry at mid rapidities. The second proces with participation of valence quarks in decuplet state in proton leads to production of baryon number with rapidity of sea quark. Two of valence quarks from proton are accompanied by quark from photon symmetric baryon fluctuation by specific configuration of gluonic fields (see Figure 9 - right). Baryon in the final state has rapidity independent from rapidity of valence quark. Rapidity of this baryon is proportial to rapidity of the sea quark. So one can predict rapidity independence of this proces. The proces is called gluonic mechanism of baryon number transport. The depence of baryon number transfer through the rapidity interval Δy using this proces is uniform and proportial to *4-5%*.

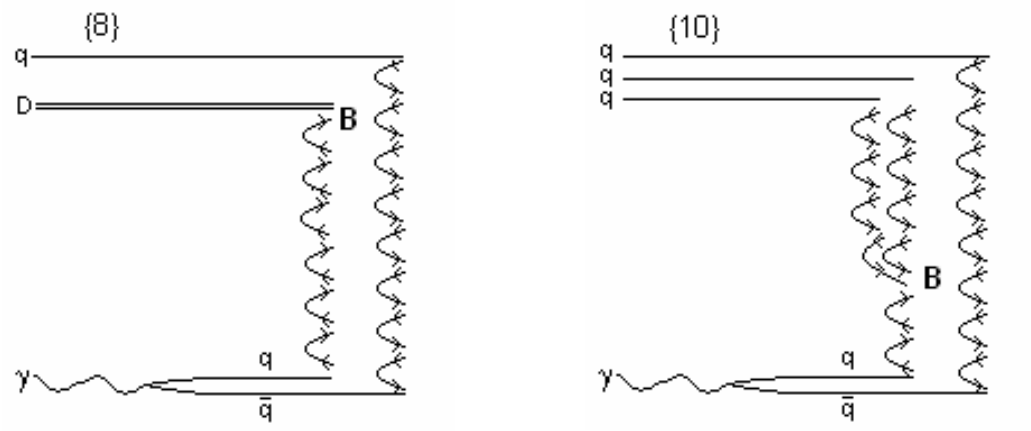

Figure 2.9: The incident photon develops a baryon number - symmetric fluctuation. Annihilation of the anti -baryon number of the fluctuation with the target leads to baryon asymmetry in the photon fragmentation region. When the target proton is in the octet color state {8}, baryon number is produced with rapidity of valence quark - quark mechanism of baryon number transport (left). When the target proton is in the decuplet color state {10}, baryon number is produced with rapidity of sea quark - gluon mechanism of baryon number transport (right).

The two mechanisms can be distinguished by the dependence of A_{BN} on the multiplicity n of produced particles. An important signature of the gluonic mechanism is a higher multiplicity of produced particles. This is due to three string topology of the final state. The valence quark exchange mechanism exibits two string topology. It is easy to see in Figure 9 that the mean multiplicity of produced particles in the rapidity interval where the baryon asymmetry is measured is *5/4* times larger for the gluonic mechanism compared to the quark exchange mechanism. This fact makes baryon asymmetry dependent on the multiplicity of the produced hadrons.

Now some experimental results. A sizeable baryon - antibaryon asymmetry in photon - proton interaction was observed by the H1 collaboration for protons and antiprotons with small momentum in the laboratory frame produced in γp collisions at HERA. The preliminary data presented at Vancouver Conference [26] show that

$$A = 2\frac{N_p - N_{\bar{p}}}{N_p + N_{\bar{p}}} = (8.0 \pm 1.0 \pm 2.5)\%, \tag{1.8}$$

where $N_p, N_{\bar{p}}$ are the number of detected protons and antiprotons. Obviously, the observed excess of protons is a consequence of the presence of proton baryon number in the initial state of the reaction. Nontrivial is however the very large rapidity interval about *8* units between intial and final protons. This can be explained by gluonic mechanism of baryon transport which is explained on the top.

Also dependence of asymmetry of produced particles on asociated multiplicity was calculated and measured by the H1 collaboration. The data agree well with the assumption that the baryon asymmetry is dominated by the contribution the gluonic mechanism, but reject any sizeable contribution of the valence quark mechanism wnich leads to a constant asymmetry.

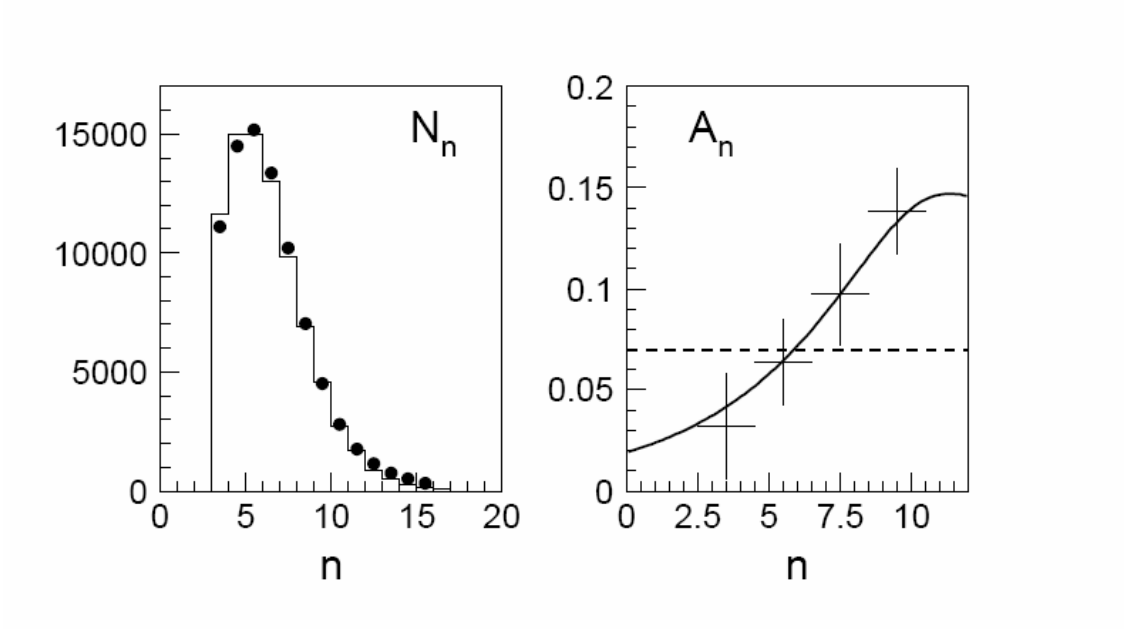

Figure 2.10: Multiplicity distribution of charget hadrons produced in photon proton interaction as measured by H1 collaboration at HERA. The histigram represents the data, the black points are the results of calculations [27] (left).

Baryon number asymmetry as function of multiplicity of charged hadrons. The crosses are the results of measurements at HERA [26]. The solid and dashed curves show the prediction for the gluonic and valence quark exchange mechanism respectively (right).

1.3 Baryon number flow in proton - proton collisions

Let us consider an ultra - relativistic pp colision in its center - of - mass frame, which coincides with the lab frame in collider experiments. At sufficiently high energies, the valence quark distribution will be Lorentz - contracted to thin pancakes with thickness (1.9)

$$z_V \cong \frac{1}{x_V P},$$

where P is the c. m. momentum in the collision, and $x_v \sim 1/3$ is a typical fraction of the proton`s momentum carried by valence quark. The typical time needed for the interaction of valence quarks from different protons with each other during collision is given by the characteristic interquark distance in impact parameter plane,

$$t_{\text{int}} = const \approx 1\, fm. \tag{1.10}$$

However, the time available for this interaction in the collision is only

$$t_{coll} \approx z_V \cong \frac{1}{x_V P}, \tag{1.11}$$

It is therefore clear that at sufficiently high energies when $t_{coll} << t_{int}$, the valence quarks of the colliding protons do not have time to interact during collision and go through each other, populating the fragmentation regions. In the conventional picture, the baryon number follows the valence quarks.

At first glance the argument looks correct, and is well supported experimentaly - leading effect for baryons in high energy pp colisions is well established. However the structure of baryon gluonic fields suggests that this scenario may not be entirely consistent. As we have stressed above the trace of baryon number has to be associated with string junction. The string junction contains an infinite number of gluons which threfore by virtue of momentum conservation should carry on the average an infinitely small fraction $x_s << x_v$ of the proton`s momentum. We therefore expect that the string junction configuration may not be Lorenz contracted to a thin pancake even at asymptotically high energies, since

$$z_S \cong \frac{1}{x_S P} >> z_V . \tag{1.12}$$

In this case the string junction will always have enough time to interact, and we may expect to find stopped baryons in the central rapidity region even in a high energy collision. This argument leads to a peculiar picture of a high energy pp collision: in some events, one or both of the string junction are stopped in the central rapidity region whereas the valence quarks are stripped off and produce three jet events in the fragmentation regions. Immediately after collision the central region is then filled by a gluon sea containing one or two twists which wil later on be dressed up by sea quarks and will form baryons. Note that the quark compositon of the produced baryons wil in general differ from the composition of colliding protons.

Why then is the leading baryon effect o gross feature of high - energy *pp* collisions? The reason may be following. The string junction, connected to all three of the valence quarks, is confined inside baryon, whereas pp collisions become on the average

more and more peripheral at high energies. Therefore in typical high - energy collision, the string junctions of the colliding baryons pass far away from each other in the impact parameter plane and do not interact. One can however select only central events, triggering on high multiplicity of the produced hadrons. In this case, we expect that the string junctions will interact and may be stoped in the central rapidity region. Even at very high energies there should be more baryons than antbaryons.

Let`s now turn to the consideration of baryon stopping in *pp* collisions. The relevant diagrams are shown in Figures 11, 12 and 13. We consider the simultaneous stopping of the two string junction in the central rapidity region, accompanied by three - jet events in the fragmentation regions and the stopping of the string junction of one proton in the soft parton field of the other, accompanied by one three jet event. Also the event without baryon stopping in central rapidity region is showed.

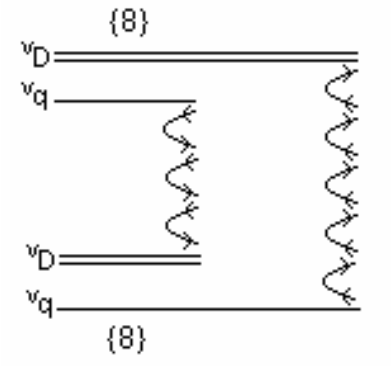

Figure 2.11: Event without string junction stoping in central rapidity region. Both protons are in octet {8} color state, therefore only valence quark mechanism of baryon number transport is accompanied with this process. This event dont contribute to baryon number assymetry at central rapidity. You can see two string topology related with valence quark mechanism.

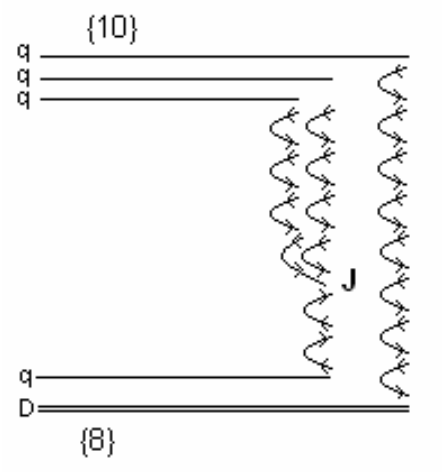

Figure 2.12: Event with stopping of the string junction of one proton in the soft parton field of the other. One proton is in octet {8} and the second in decuplet {10} color state therefore the gluonic mechanism of baryon number and also valence quark mechanism is in action. String junction (J) with rapidity of sea quark is made. This event will contribute to baryon asymmetry at central rapidity if rapidity of sea quark falls to central rapidity region.

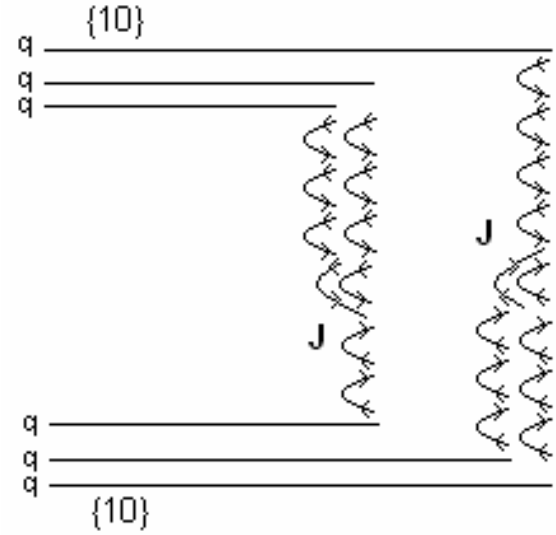

Figure 2.13: Event with stopping of both string junctions. Both protons are in decuplet {10} color state therefore only gluonic mechanism of baryon number transport is acommpanied with this process. Baryon number equal two can be pushed in the central rapidity region, but propabilityof this kind of event is very low (~0.01%)

2 Expectation at ALICE

Monte Carlo data are representing real physics. There are many diferent theoretical models and also many diferent monte carlo generators for high energy physics. In this chapter we are discussing differences between results from so called “standard” Monte Carlo generators (Pyhia, Hijing, Herwig) and “special” Monte Carlo generator Hijing B. “Standard” generators are representing models without string junction transfer. Differences between these generators are discussed bellow. Hijing B implement model with string junctions, so non vanishing asymmetry should be seen in central rapidity region.

For every generator was made baryon number asymmetry (2.7) and ratio plots for protons and Λ hyperons at colision energies 900 GeV and 14 TeV. Only baryons in Alice acceptation $|\eta|<1$ region was chosen. For Hijing B generator also overall rapidity ($|\eta|<7$) plots are shown. 100 000 events was processed for every generator.

2.1 PYTHIA

PYTHIA [50] [51] can generate different types of high-energy physics events. It is based on perturbative QCD but also includes models of soft interactions, parton showers and multiple interactions, fragmentation and decays.

Owing to the composite nature of hadrons, several interactions between parton pairs are expected to occur in a typical hadron–hadron collision [52]. Evidence for these interactions has mounted including their direct observation by CDF [53]. However, the understanding of multiple interactions is still primitive. Therefore, PYTHIA contains four different models as options available to users. The main parameter in these models is *p*t min, a cut-off introduced to regularize the dominant 2→2 QCD cross sections, which diverge as $p_t \to 0$ and drop rapidly at large p_t. Apart from the default Model 1, all other models assume a continuous turn-off of the cross section at p_t min. Models 3 and 4, originally developed to fit the UA5 data, assume a varying impact parameter between the colliding hadrons. The hadronic matter distributions are assumed to have Gaussian (Model 3) or a double Gaussian (Model 4) shapes. Several studies have concluded that

such models provide a better description of the UA5 multiplicity distributions than Model 1 [54] [55], The Gaussian-type models also better describe the underlying production in beauty events at the Tevatron [56].

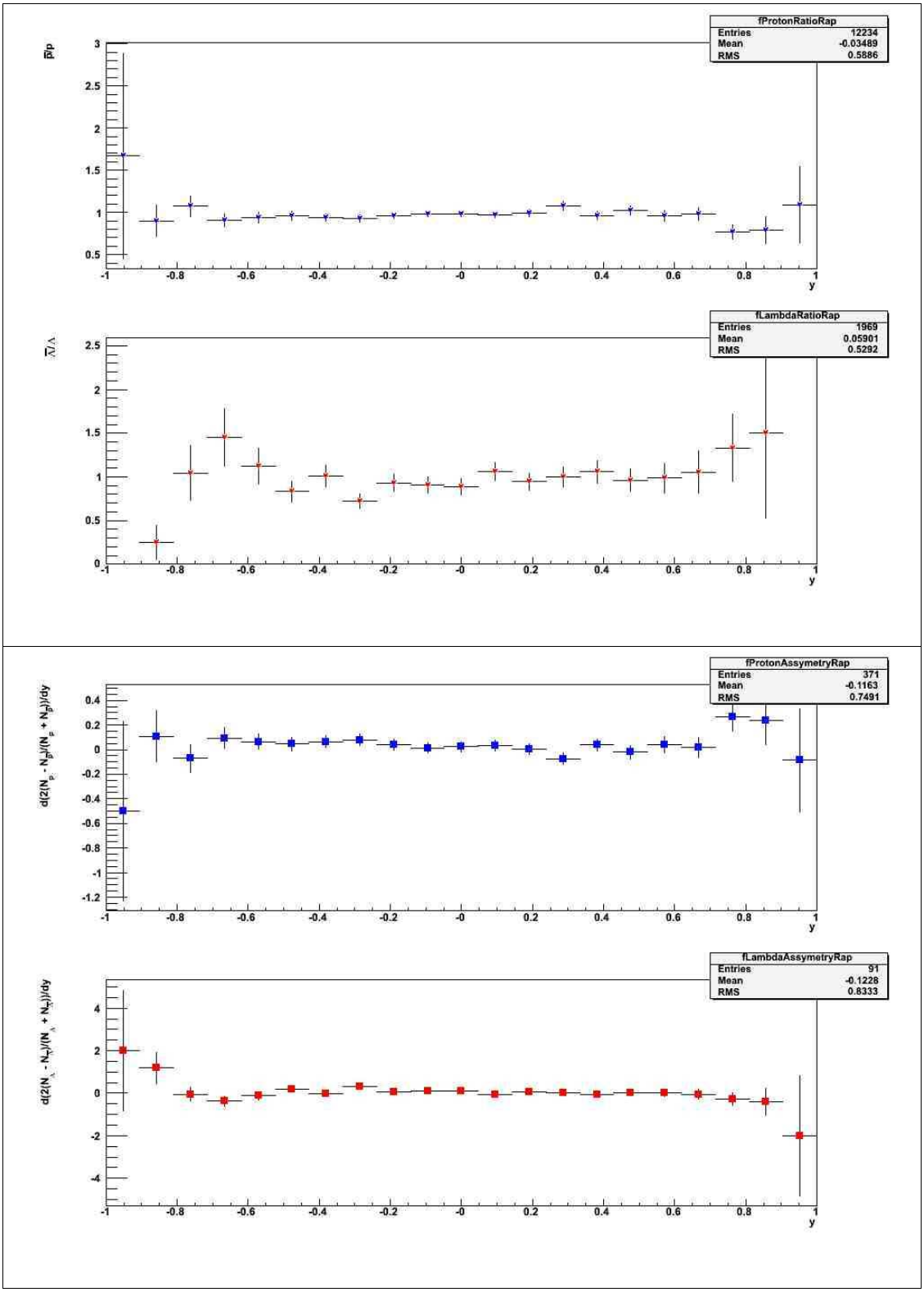

Figure 4.1: Ratio (up) and Asymmetry (down) plot in central rapidity for protons (blue) and lambdas (red) from Pythia 6 generator. Energy of collision = 900 GeV.

2.2 HIJING B

HIJING B [60] [61] modifies the HIJING event generator to include both the baryon junction exchange mechanisms for baryon number transport and baryon pair production. These mechanisms are modeled by new string con figurations which are added to the two qq - q string background. This event generator is OSCAR compatible [62].

Modifications to HIJING: Several subroutines were added to HIJING. The parameters associated with the junction mechanisms and those associated with string fragmentation were tuned to reproduce the p + p data at p_{lab} = 400 GeV/c [63] and p + S collisions at p_{lab} = 200 GeV/c [64]. The common block which holds the parameters for the junction mechanisms is called HIJB.

The main subroutines which were added to HIJING are called HIJBJE and HIJBAB. HIJBJE simulates the junction exchange by breaking a string into a baryon and three jets. HIJBAB simulates the J loops by breaking a string into a baryon, antibaryon and several jets.

In order to reproduce the p + p 400 GeV/c data, several string fragmentation parameters were adjusted. The parameter P_{qq-q} = parj(1) which describes the probability for producing diquark to quarks is adjusted from 0.10 to 0.02. The probability for producing s quarks to u and d quarks, $P_{s/u}$ = parj(2) is adjusted from 0.30 to 0.23 and the extra suppression of the diquarks, parj(3) is adjusted from 0.40 to 0.70.

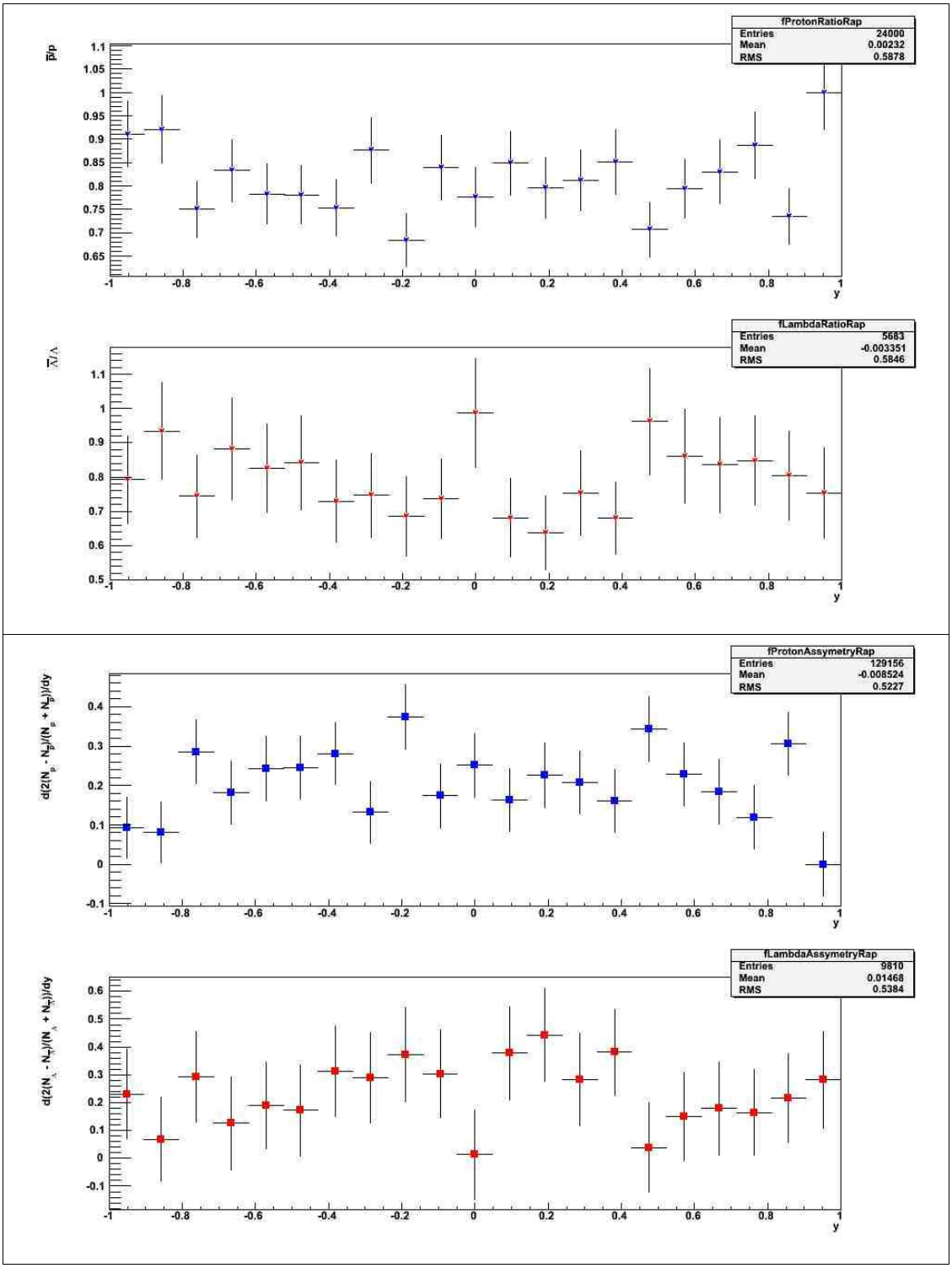

Figure 4.7: Ratio (up) and Asymmetry (down) plot in central rapidity for protons (blue) and lambdas (red) from Hijing-B generator. Energy of collision = 900 GeV.

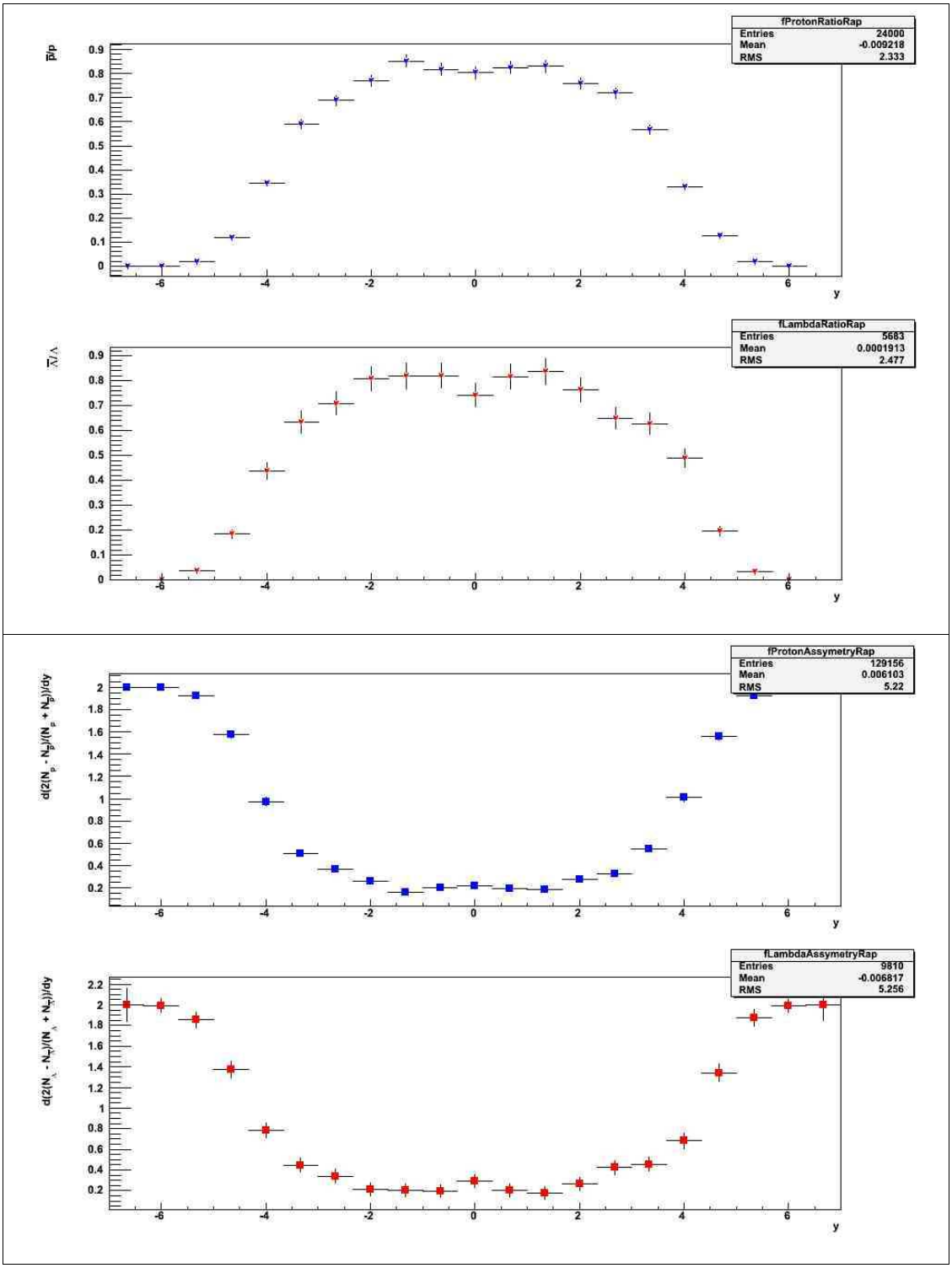

Figure 4.9: Ratio (up) and Asymmetry (down) plot in overall rapidity for protons (blue) and lambdas (red) from Hijing-B generator. Energy of collision = 900 GeV.

2.3 Comparison

As was expected – you can see vanishing asymmetry in central rapidity region for generators PYTHIA. This generator do not include string junction stopping mechanisms. It represents model where the baryon number of the incident proton is associated with valence quarks and transferred to a more central rapidity region by diquark exchange the mechanism is attenuated exponentially with the rapidity interval over which the baryon charge is moved.

For HIJING – B you can see nonzero asymmetry in central rapidity region. This is caused by fact that in HIJING - B baryon number is carried by gluonic field, baryon number flow can be due to a purely gluonic mechanism. This is accounted for in models where the three valence quarks of the proton fragment independently but are joined by strings to a baryonic gluon field configuration at more central rapidity, the string junction.

Effect of string junction transfer which has rapidity independent distribution becomes dominant in central rapidity region, where another effects vanishes. This can be pretty seen on overall rapidity histograms (see Figures 4.9, 4.10).

3 Corrections

3.1 The Correction Framework

The classes that have been developed so far with the purpose of assisting the ALICE users in deriving the corrections for their analyses can be grouped into two main categories:

• “Container” Classes

• “Selection” Classes

which reflect the main utilities provided by the Correction Framework (CF):

- The possibility to store, while performing analysis, both real and simulated data over binned N dimensional grids, to then derive the efficiency correction maps and correct the observed data.

- The coding of general selections which may be common to several analyses, at different stages of the selection process (for example, generator, acceptance, reconstruction, user-specific analysis selection...), with the optional possibility of accumulating control histograms on the selection variables (intended to be the base for the user to perform the correction “QA”).

In the following, some information is given on the structure of the code and its functionalities.

3.2 The correction process flow

Flow of the correction process is the following: We will first loop over simulated data and accumulate information on the 2-dimensional y-P_T grids using AliCFContainer-type object, in order to derive the overall efficiency correction and also monitor its components (the reconstruction efficiency, the PID efficiency).

We are using 3-level AliCFContainer with these stages: Selected Monte Carlo particles (protons), reconstructed proton tracks, identified protons. Following criteria (cuts) are used to choose inputs to the stages (see Figure 5.1):

- Selected Monte Carlo particles: Primary protons with rapidity -1< y <1 and transverse momentum 0.1< P_T <3.1.
- Reconstructed proton tracks: Tracks which belongs to “Selected MC particles”. To choose these tracks we are using *TParticle::GetLabel()* function. Multiple tracks are excluded and several cuts are applied on these tracks (see Cuts).
- Identified protons: Tracks from “Reconstructed proton tracks” which are identified as a protons.

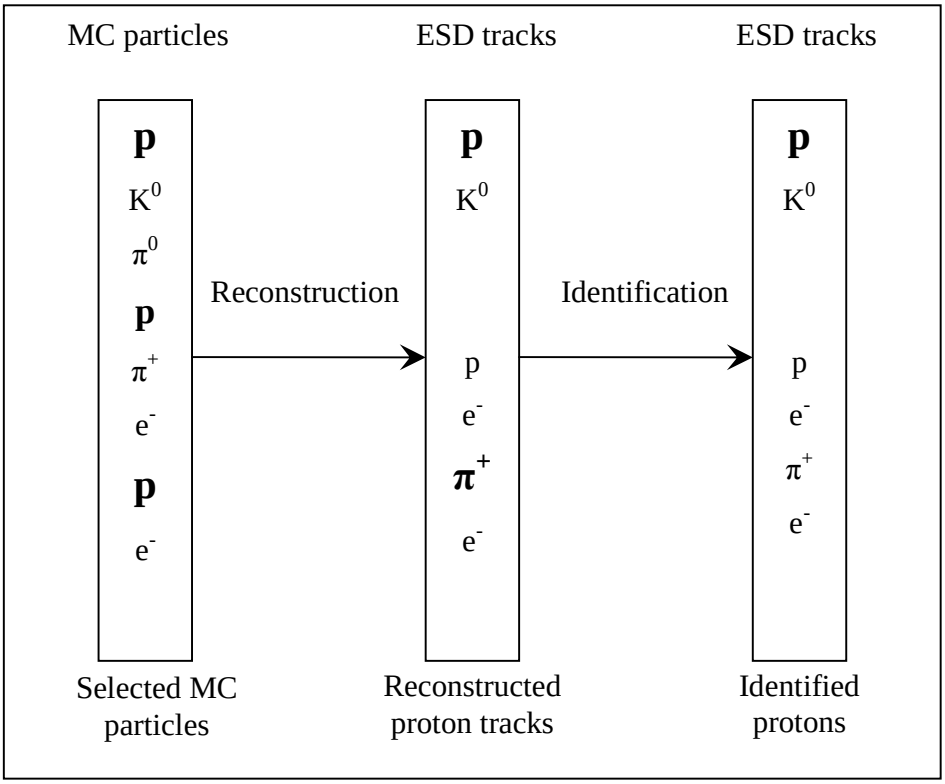

Figure 5.1: Example showing selection to three container stages. Bold printed particles (tracks) are selected

The correction maps, are derived with and stored in AliCFEffGrid-type objects.

When using the real data, next flow will be the following (see Figure 5.2): AliCFEffGrid-type objects will then be used to correct the observed data (deposited on a AliCFDataGrid-type object), which were accumulated over an equivalent grid via an AliCFContainer during a separate analysis loop on real events.

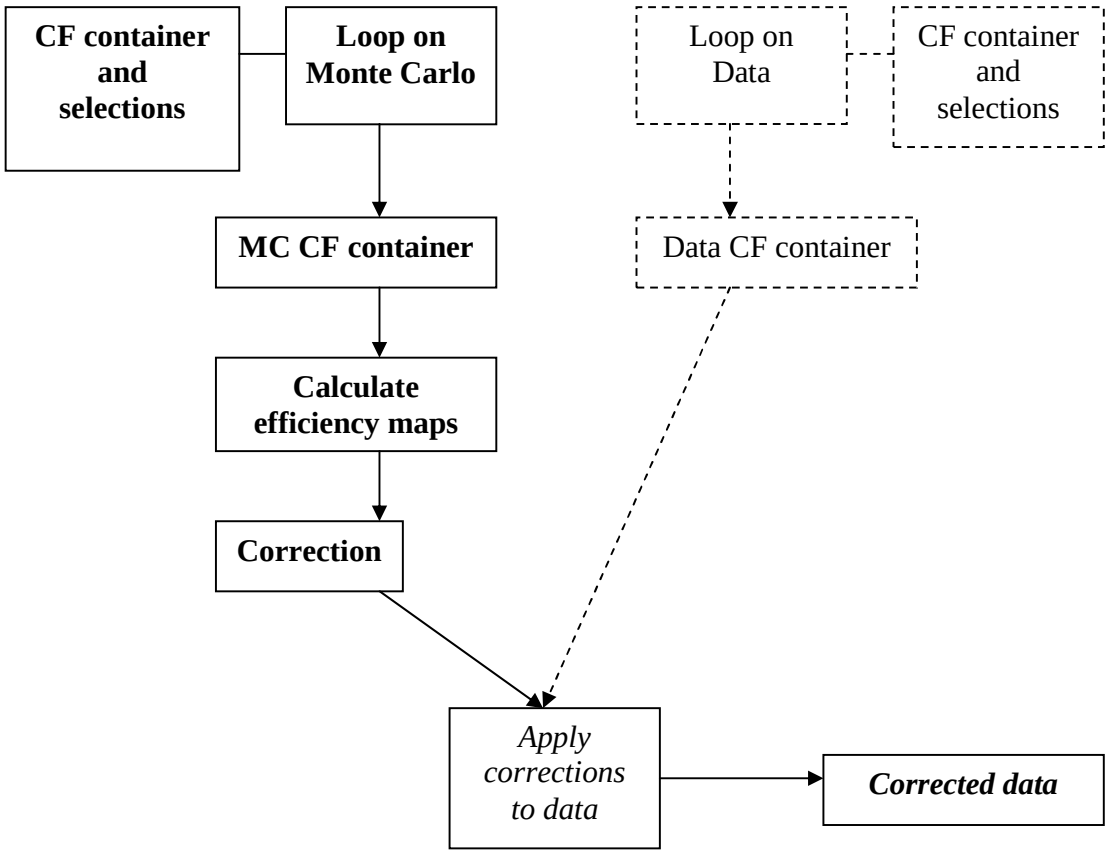

Figure 5.2: Schema showing correction process flow with real data. Left branch (printed bold) is shown in more detail in Figure 5.3. Steps which are printed italic are different in correction process with MC-only. Steps in dashed boxes do not exist in correction process with MC-only.

Because we are working only with Monte Carlo next flow is different (see Figure 5.2 and 5.3). We apply corrections directly to Identified protons which were accumulated in MC CF container.

We are using PDC 07 ESD files. They are reconstructed PYTHIA6 events for collisions energy 900 GeV. 28000 events was processed.

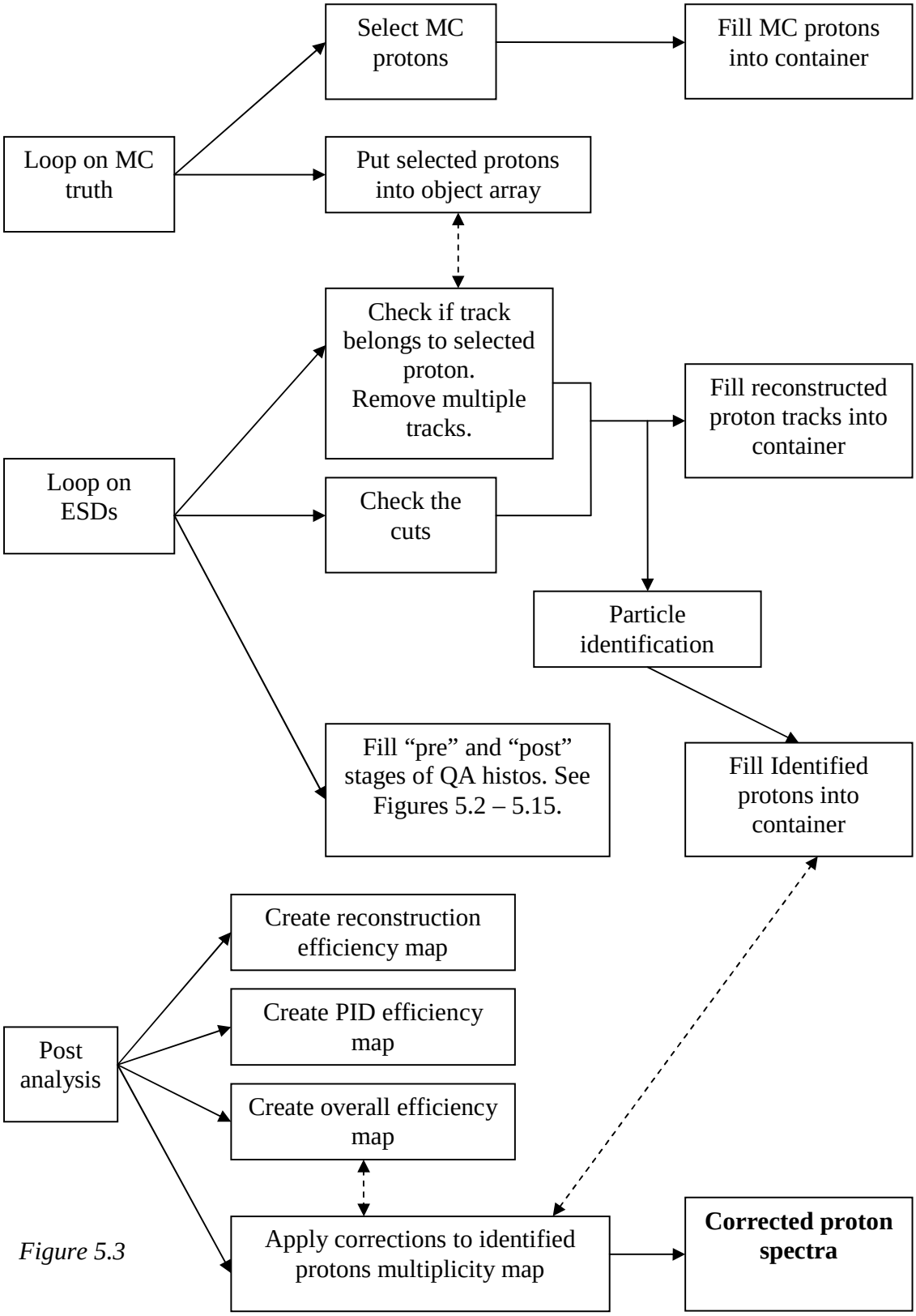
Select MC protons
Fill MC protons into container
Loop on MC truth
Put selected protons into object array
Check if track belongs to selected proton. Remove multiple tracks.
Fill reconstructed proton tracks into container
Loop on ESDs
Check the cuts
Particle identification
Fill "pre" and "post" stages of QA histos. See Figures 5.2 – 5.15.
Fill Identified protons into container
Create reconstruction efficiency map
Create PID efficiency map
Post analysis
Create overall efficiency map
Apply corrections to identified protons multiplicity map
Corrected proton spectra

Figure 5.3

3.3 Monte Carlo data

Selection of monte carlo data is a product from MC truth loop (see Figure 5.3). Monte carlo data are filled by selected MC protons (see Figure 5.1). We selected primary protons with rapidity -1< y <1 and transverse momentum 0.1< P_T <3.1.

Multiplicity is meanly constant in rapidity scale and rise strongly from high p_t to low p_t. Multiplicity at low p_t is ordinal higher than multiplicity at high p_t. See Figure 5.4.

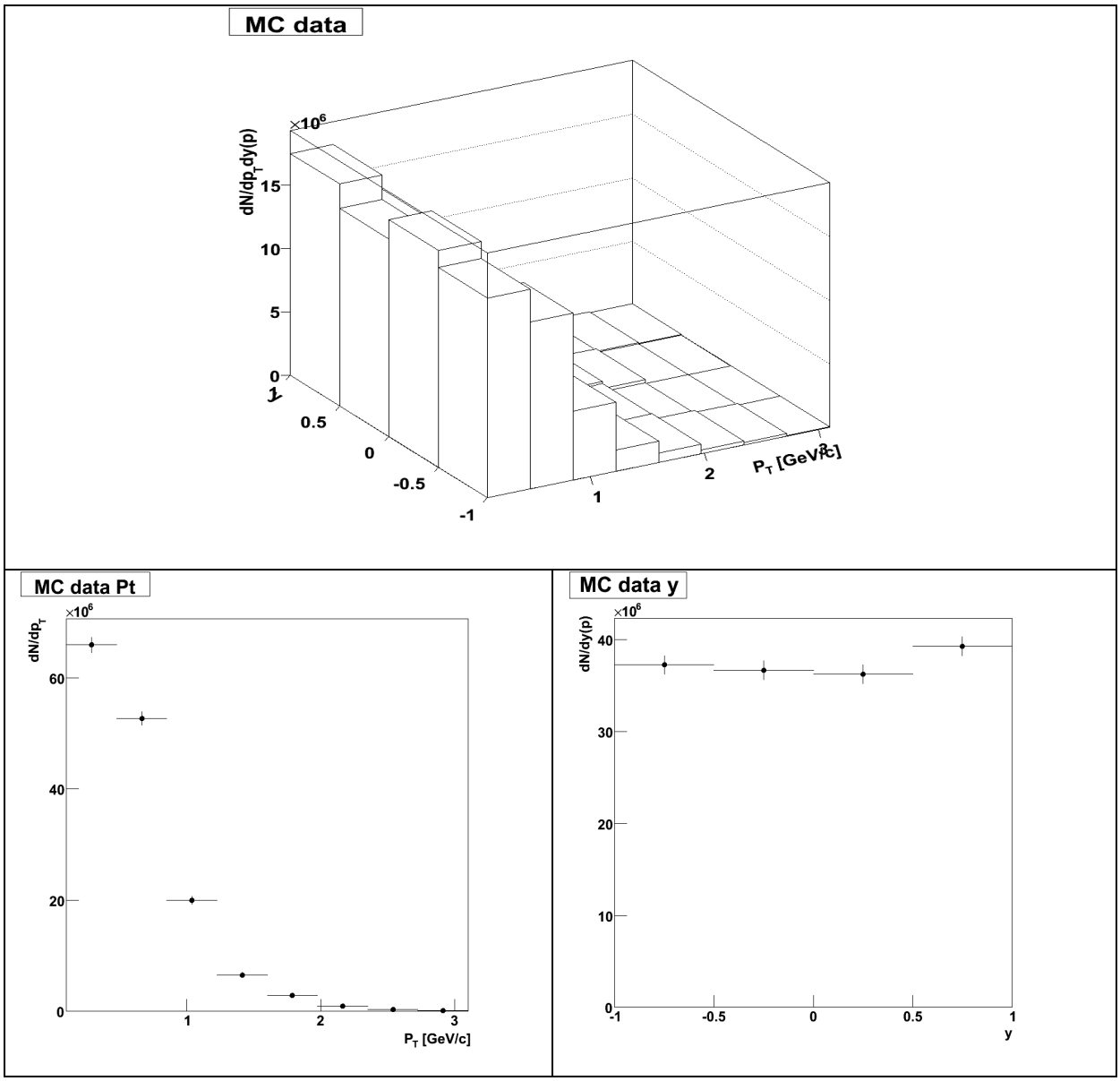

Figure 5.4: Plots showing multiplicity of primary protons – $dN/dy.dp_T$ (up) and its projections dN/dy (down left) and dN/dp_T (down right).

3.4 Cuts

Several cuts were applied on reconstructed proton tracks (see Table 5.1).

	Minimum	Maximum
Rapidity	-1	1
Transverse momentum	0.1	3.1
Number of TPC clusters	50	-
Number of ITS clusters	1	-
Chi squared per TPC cluster	-	3.5
Covariance matrix element Σ_{11}	-	2.0
Covariance matrix element Σ_{22}	-	2.0
Covariance matrix element Σ_{33}	-	0.5
Covariance matrix element Σ_{44}	-	0.5
Covariance matrix element Σ_{55}	-	2.0
Number of sigma to vertex	-	3

Table 5.1: Cuts

3.5 ESD data

Selection of ESD data is a product from ESD loop (see Figure 5.3). ESD data are filled by identified protons (see Figure 5.1). Identified protons are reconstructed proton tracks which are identified as a protons. Reconstructed proton tracks are tracks, which belongs to “Selected MC particles”. To choose these tracks we are using *TParticle::GetLabel()* function. Multiple tracks are excluded and several cuts are applied on these tracks (see Cuts).

Multiplicity is rises in rapidity scale from high |y| to central rapidity. It behavior is constant in all p_t scale. Multiplicity rise strongly from high p_t to low p_t as it was in multiplicity of monte carlo particles, but it is strongly suppressed at very low p_t. Multiplicity at low p_t is ordinal higher than multiplicity at high p_t. See Figure 5.17.

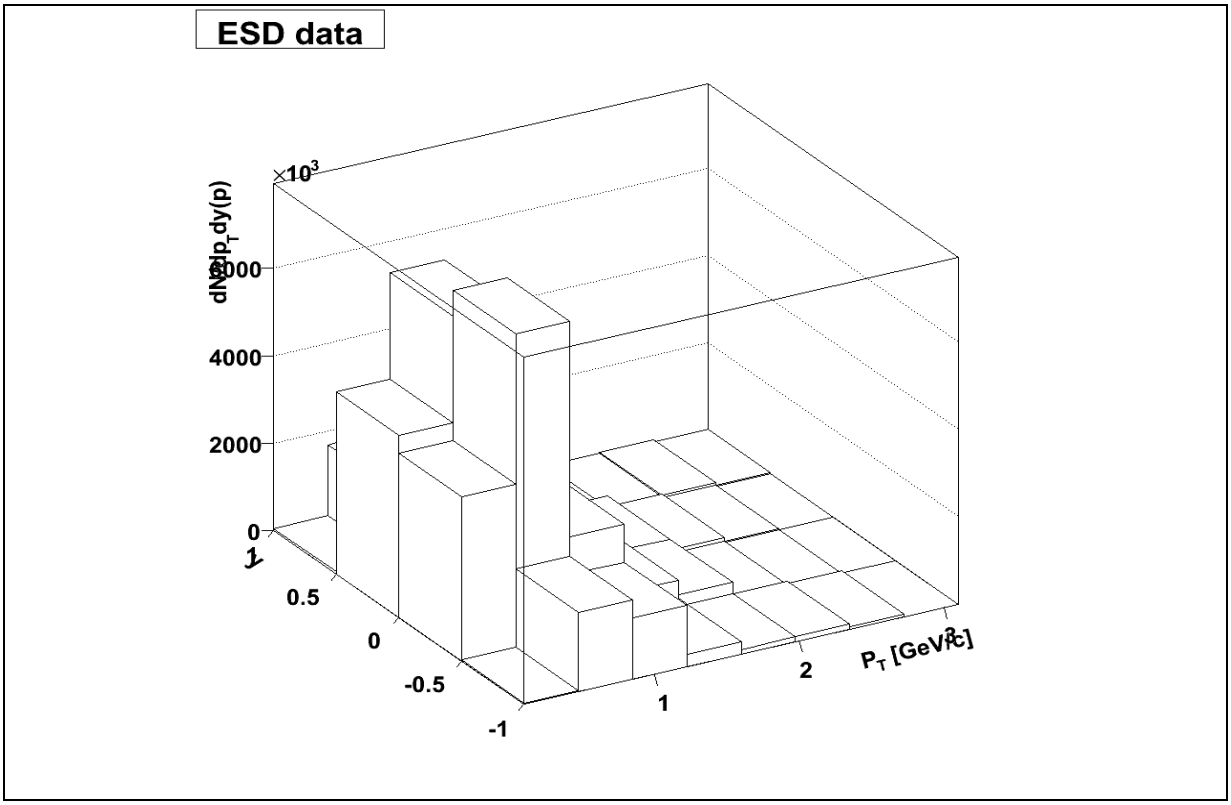

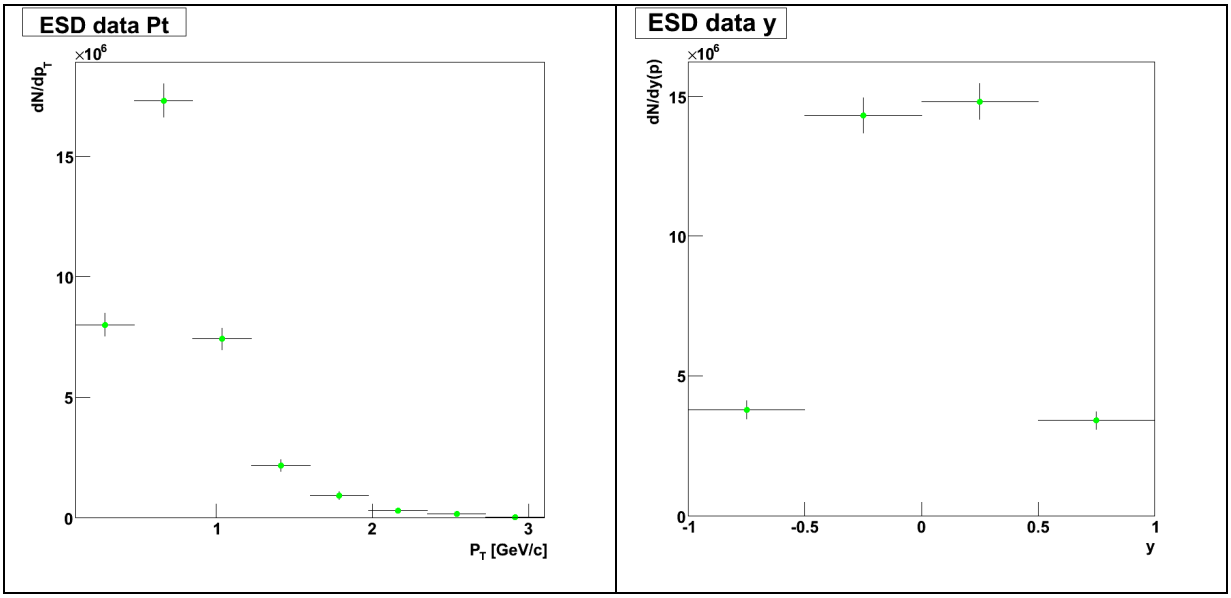

Figure 5.17: Plots showing multiplicity of identified proton tracks – $dN/dy.dp_T$ (up) and its projections dN/dy (down left) and dN/dp_T (down right).

3.6 Monte Carlo and ESD data – comparison

Because of cuts applied on ESD tracks, reconstruction process and identification, the multiplicity of ESD protons is different for multiplicity of selected MC protons (see Figure 5.18).

Absolute value of multiplicity is suppressed everywhere in y-p_t scale. Shapes of MC data distribution and ESD data distribution are different. We can see reasonable decrease at high p_t and high |y|. Corner bins: y-p_t very high are ordinary suppressed in ESd data.

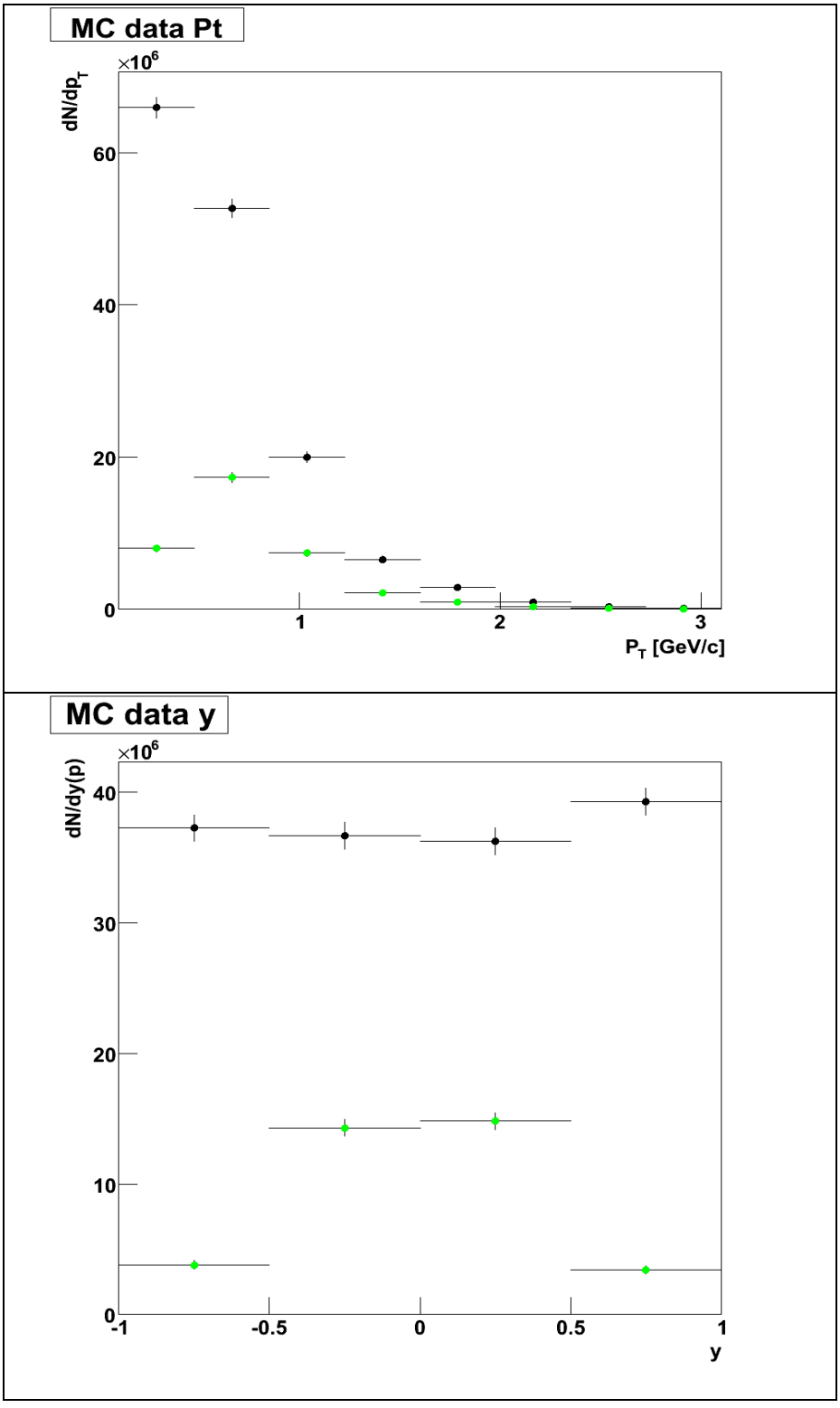

Figure 5.18: Comparison of multiplicities of identified proton tracks (green) and primary protons from Monte Carlo (black).

3.7 Efficiency

Process of creating the efficiency maps is a part of post analysis (see Figure 5.3). We created three efficiency maps: Reconstruction efficiency, PID efficiency and overall efficiency.

- Reconstruction efficiency: Map is obtained by dividing the reconstructed proton tracks multiplicity by selected MC particles multiplicities. It describes only quality of track reconstruction process itself. Efficiency is rising in p_t scale from low values at low p_t to almost 1 at high p_t. In y scale is efficiency lower at high |y| and higher in central rapidity region. See Figure 5.19 up.
- PID efficiency: Map is obtained by dividing the identified protons multiplicity by reconstructed proton tracks multiplicity. It describes quality of particle identification procedure itself without track reconstruction quality. Distribution is meanly constant, in rapidity and also in p_t. Particle identification is almost 1 in y-p_t region we are investigating. See Figure 5.19 middle.
- Overall efficiency: Map is obtained by dividing the identified protons multiplicity by selected MC particles multiplicity. It describes quality of whole process – track reconstruction and particle identification. We can say that it describes quality of particle reconstruction process. This efficiency map can be also obtained as a product of reconstruction efficiency and PID efficiency. Surface of this distribution is similar to surface of reconstruction efficiency distribution only absolute values are little bit lower because of PID. See Figure 5.19 down.

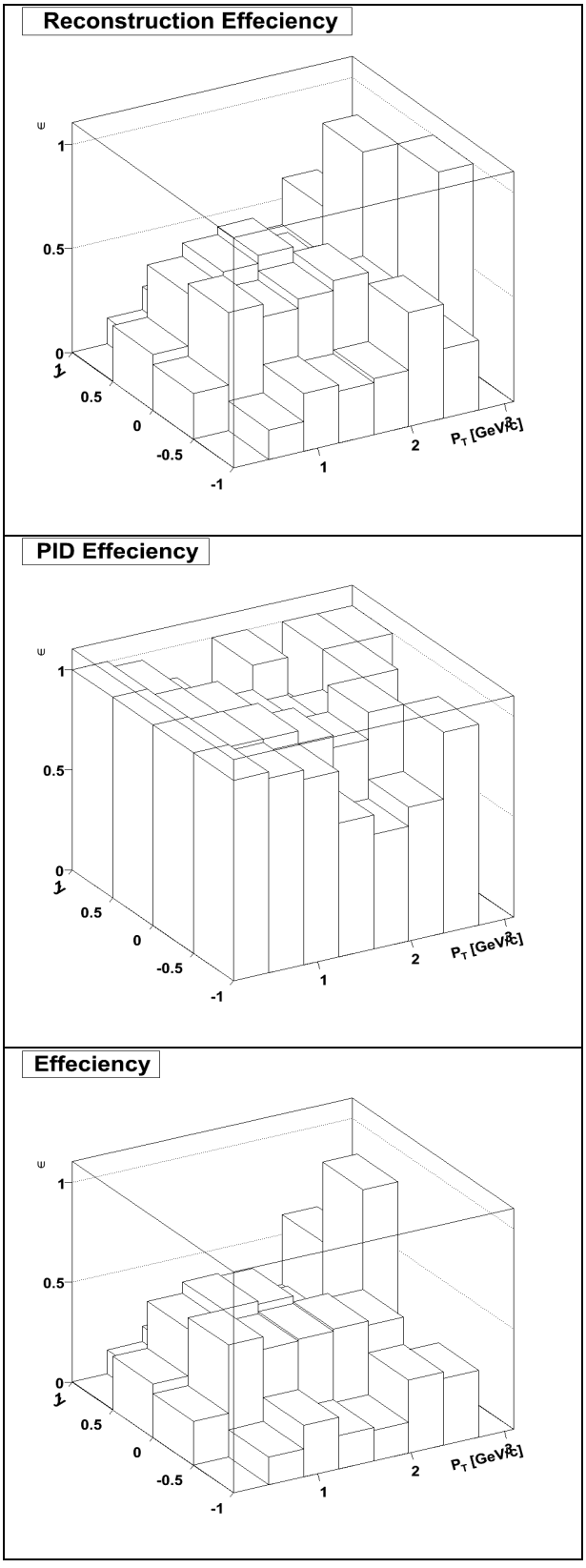

Figure 5.19: Plots in y-p_T for reconstruction efficiency (up) particle identification efficiency (middle) and overall efficiency (down).

3.8 Corrected ESD data and Monte Carlo data – comparison

Corrected ESD data are made by applying corrections on track reconstruction efficiency and particle identification efficiency on ESD data. We are doing it at one bout with overall efficiency map (See Figure 5.19 down). Correction map is inverse distribution to efficiency. Corrected ESD data is then made as a product of uncorrected ESD data (Figure 5.4) and correction map.

Comparison is crucial because we want to get MC truth multiplicities from this. Because it is self correction we should get the same distribution as from MC data.

And we did. See Figure 5.20.

It is important to have good statistic when producing correction map. When some bin in ESD data distribution is empty all information about multiplicity is lost and in correction map (efficiency also) will be an empty bin. Then after correction in corrected ESD data will be also empty bin and in MC data can be for example 1000 inputs. This problem can appear for corner bins with low p_t and high |y|. In this region multiplicity is hardly suppressed and overall efficiency is very low, as discussed before. This problem can appear also for high p_t bins where multiplicity is low also for MC data, but effect is not so bad, because number of lost particles is small. Due to small MC data multiplicity in this region.

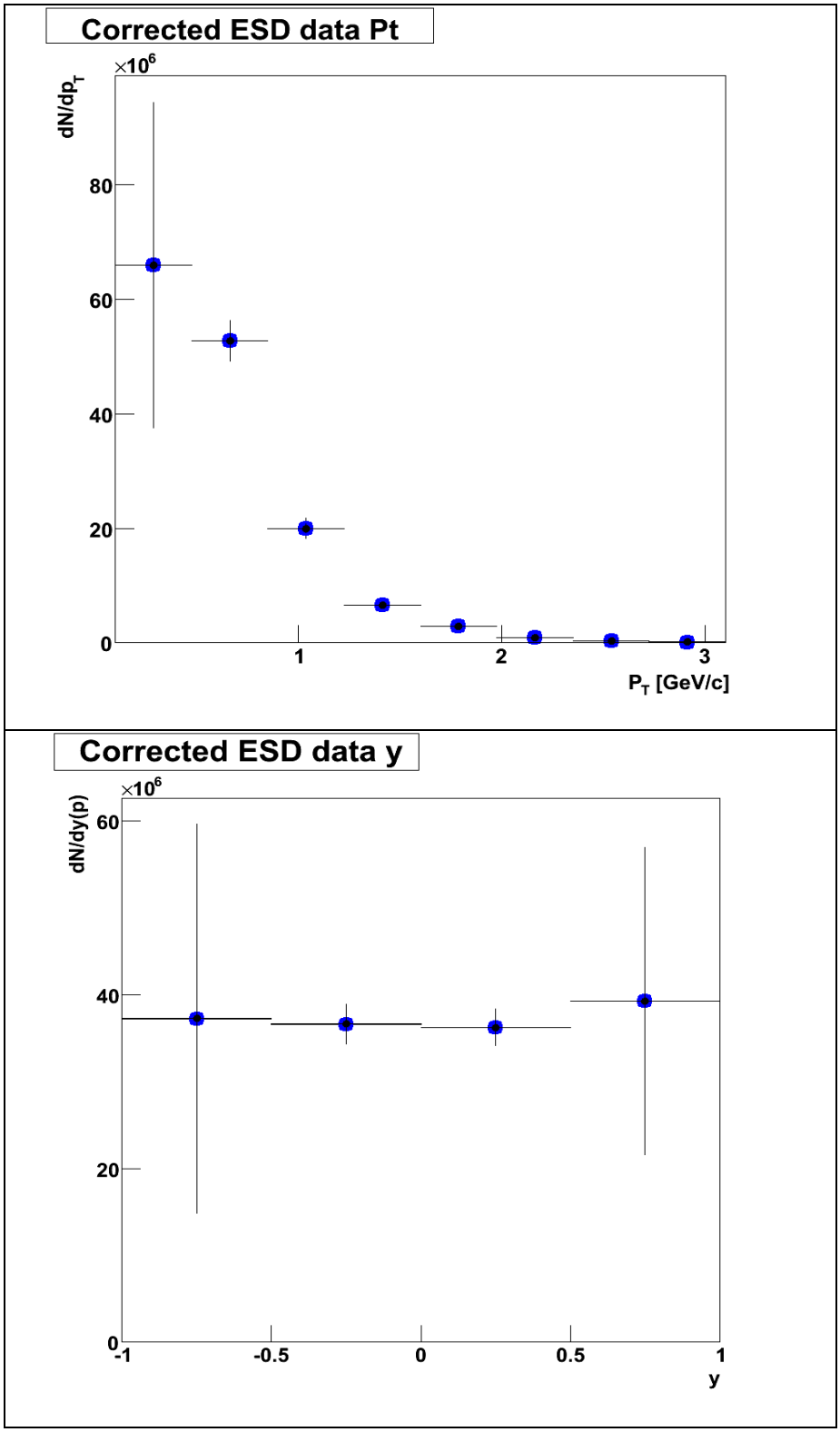

Figure 5.20: Comparison of corrected multiplicity of identified proton tracks (blue) and primary protons multiplicity from Monte Carlo (black).

Conclusion

Role of ALICE experiment and its baryon program was briefly described in chapter 1. Description of ALICE detector system with view to particle reconstruction and identification process, which is crucial for aim of this thesis, was done in chapter 3.

Detailed theoretical overview was done in chapter 2. We summarized few arguments for theory of string junction as carrier of baryon number. Previous experimental results from H1 collaboration corresponds with this.

Let us recall that described numbers of asymmetry for “string junction stopping” events depends on used model.

Study of different numerical models represented by four monte carlo generators was done. As was expected – you can see vanishing asymmetry in central rapidity region for generators PYTHIA, HIJING and HERWIG. For HIJING – B you can be seen nonzero asymmetry in central rapidity region. . This is caused by fact that in HIJING - B baryon number is carried by gluonic field, baryon number flow can be due to a purely gluonic mechanism. This is only one relevant change in HIJING – B code.

In this thesis the study of particle reconstruction and identification effects to proton/antiproton multiplicity was done. Cuts made inside of reconstruction process were also investigated with aspiration to choose the cuts values properly. Effects of cuts were plotted. We made efficiency and correction maps for protons/antiprotons. Corrected multiplicity spectra can be used to derive asymmetry plots and to see asymmetry in central rapidity which is not distorted by systematical effects.

Literature

[1] Giubellino P et al 2000 ALICE Internal Note 2000-28; Revol J-P 2002 Proc. 3rd Int. Symp. on LHC Physics and Detectors, EPJ Direct C 4 (S1) 14,

[2] Giovannini A and Ugoccioni R 1999 Phys. Rev. D 60 074027

[3] Giovannini A and Ugoccioni R 1999 Phys. Rev. D 59 094020

[4] Acosta D et al [CDF Collaboration] 2002 Phys. Rev. D 65 072005

[5] Van Hove L 1982 Phys. Lett. B 118 138

[6] Alexopoulos T et al [E735 Collaboration] 1990 Phys. Rev. Lett. 64 991

[7] Alexopoulos T et al [E735 Collaboration] 1993 Phys. Rev. D 48 984

[8] Becattini F et al 2001 Phys. Rev. C 64 024901

[9] Kopeliovich B Z and Zakharov B G 1989 Z. Phys. C 43 241

[10] Kopeliovich B Z and Povh B 1999 Z. Phys. C 75 693 Kopeliovich B Z and Povh B 1999 Phys. Lett. B 446 321

[11] Rossi G C and Veneziano G 1997 Nucl. Phys. B 123 507. Rossi G C and Veneziano G 1980 Phys. Rep. 63 149

[12] Calucci G and Treleani D 1998 Phys. Rev. D 57 503

[13] Calucci G and Treleani D 1999 Phys. Rev. D 60 054023

[14] Kaidalov A B 1979 Phys. Rep. 50 157

[15] Alberi G and Goggi G 1981 Phys. Rep. 74 1

[16] Goulianos K 1983 Phys. Rep. 101 169

[17] Martin A D 2001 Preprint hep-ph/0103296

[18] Kaidalov A B, Khoze V A, Martin A D and Ryskin M G 2001 Eur. Phys. J. C 21 521

[19] Abe F et al [CDF Collaboration] 1997 Phys. Rev. Lett. 79 584

[20] Abe F et al [CDF Collaboration] 1997 Phys. Rev. D 56 3811

[21] A. Casher, H. Neuberger and S. Nussinov, Phys. Rev. D20 (1980) 179

[22] B. Baier et al., Nucl. Phys. B484 (1997) 265

[23] M. Vasiliev et al., Phys. Rev. Lett. 83 (1999) 2304

[24] E. Gotsman and S. Nussinov, Phys. Rev. D 22 (1980) 624

[25] V. Artry, Nucl. Phys. B85 (1975) 442

[26] The H1 Collaboration, C. Adloff et al., Measurement of the Baryon-Antibaryon Asymmetry in Photoproduction at HERA, Submitted to the 29th Int. Conf. on High-Energy Phys. ICHEP98, Vancouver, Canada, July 1998. Abstract 556.
[27] B.Z. Kopeliovich and B. Povh, Phys. Lett. B446 (1999) 321
[28] ALICE Collaboration 2000 Technical Design Report of the Time-Projection Chamber CERN/LHCC/2000–01
[29] ALICE Collaboration 1995 Technical Proposal CERN/LHCC/95–71
[30] ALICE Collaboration 1996 Technical Proposal Addendum 1, CERN/LHCC/96–32
[31] ALICE Collaboration 1999 Technical Proposal Addendum 2, CERN/LHCC/99–13
[32] ALICE Collaboration 2001 Technical Design Report of the Transition-Radiation Detector CERN/LHCC/2001–21
[33] ALICE Collaboration 2000 Technical Design Report of the Time-Of-Flight Detector CERN/LHCC/2000–12;Addendum CERN/LHCC/2002–16
[34] Cerron-Zeballos E, Crotty I, Hatzifotiadou D, Lamas-Valverde J, Neupane D, Williams M C S and Zichichi A 1996 Nucl. Instrum. Methods A 374 132
[35] Akindinov A et al 2000 Nucl. Instrum. Methods A 456 16
[36] ALICE Collaboration 1998 Technical Design Report of the High-Momentum Particle Identification Detector CERN/LHCC/1998–19
[37] Thews R L, Schroeder M and Rafelski J 2001 Phys. Rev. C 63 054905
[38] Braun-Munzinger P and Stachel J 2000 Phys. Lett. B 490 196
[39] Billoir P 1984 Nucl. Instrum. Methods A 225 352
[40] ALICE Collaboration 1999 A Transition Radiation Detector, Technical Proposal, Addendum 2,CERN/LHCC 99-13
[41] ALICE Collaboration 2001 Technical Design Report of the ALICE Transition Radiation Detector,CERN/LHCC 2001-021
[42] Andronic A et al (ALICE Collaboration) 2004 Nucl. Instrum. Methods A 519 508
[43] Aguilar-Benitez M et al 1991 Z. Phys. C 50 405
[44] Wang X-N and Gyulassy M 1991 Phys. Rev. D 44 3501

[45] Gyulassy M and Wang X-N 1994 Comput. Phys. Commun. 83 307–31
[46] Andersson B et al 1983 Phys. Rep. 97 31
[47] Andersson B et al 1987 Nucl. Phys. B 281 289
[48] Nilsson-Almqvist B and Stenlund E 1987 Comput. Phys. Commun. 43 387
[49] Capella A et al 1994 Phys. Rep. 236 225
[50] Bengtsson H-U and Sjostrand T 1987 Comput. Phys. Commun. 46 43
[51] Sjostrand T 1994 Comput. Phys. Commun. 82 74
[52] Sjostrand T and van Zijl Z M 1987 Phys. Rev. D 36 2019
[53] Abe F et al [CDF Collaboration] 1997 Phys. Rev. Lett. 79 584
[54] Alner G J et al [UA5 Collaboration] 1983 Phys. Lett. B 138 304
[55] Mangano M L and Altarelli G (ed) 2000 CERNWorkshop on Standard Model Physics (and more) at the LHC,CERN Yellow Report CERN-2002-004
[56] Abe F et al [CDF Collaboration] 1999 Phys. Rev. D 59 32001
[57] Marchesini G et al 1992 Comput. Phys. Commun. 67 465
[58] Marchesini G andWebber B R 1988 Nucl. Phys. B 310 461
[59] Webber B R 1984 Nucl. Phys. B 238 492
[60] S.E Vance and M. Gyulassy. Phys. Rev. Lett 83 (1999) 1735
[61] S.E Vance, M. Gyulassy and X.N. Wang, Phys. Lett. B443 (1998) 45
[62] http://rhic.phys.columbia.edu/rhic/
[63] M. Aguilar-Benitez et al. Z.Phys. C50 (1991) 405
[64] T. Albert et. al. (NA35 Collaboration). Z. Phys. C64 (1994) 195